CHEMICAL ENGINEERING TRANSACTIONS
VOL. 60, 2017
A publication of AIDIC
The Italian Association of Chemical Engineering
Online at www.aidic.it/cet
Guest Editors: Luca Di Palma, Elisabetta Petrucci, Marco Stoller

ISBN 978-88-95608- 50-1; **ISSN** 2283-9216
DOI: 10.3303/CET1760023

Improved Photocatalytic Properties of Doped Titanium–Based Nanometric Oxides

Marco Scarsella*[a], Maria P. Bracciale[a], Benedetta de Caprariis[a], Paolo De Filippis[a], Antonietta Petrullo[a], Lucilla Pronti[b], Maria L. Santarelli[a]

[a] Department of Chemical Engineering Materials Environment, University of Rome Sapienza, via Eudossiana 18, 00184, Rome, Italy
[b] Department of Basic and Applied Sciences for Engineering, University of Rome Sapienza, via A. Scarpa 16, 00161, Rome, Italy
marco.scarsella@uniroma1.it

Photocatalysis is considered one of the most promising technologies for applications in the environmental field especially in the abatement of water-soluble organic pollutants. In this field, titanium dioxide nanoparticles have drawn much attention recently; however, the use of this oxide presents some limitation since it allows to obtain high photoresponse and degradation efficiency only under UV light irradiation, that represents the 3 to 4% of the solar radiation, so preventing its environmental large-scale applications under diffuse daylight. In this work the photocatalytic efficiency of titanium-based oxides systems containing alkaline earth metals such as barium and strontium, prepared by a simple sol-gel method was investigated, evaluating the degradation of methylene blue as model compound under UV and visible light irradiation. The results were compared with those obtained with Degussa P25 titanium dioxide. The achieved degradation percentage of methylene blue are very promising showing that under visible light irradiation it is possible to obtain a maximum dye removal percentage ~ 50 % higher than that obtained with the Degussa P25.

1. Introduction

The abatement of organic pollutants produced by several sectors of chemical industry is nowadays a big issue to be solved; different methods to face this problem have been proposed (de Caprariis et al., 2015; de Caprariis et al., 2014). Between them photocatalysis is one of the most promising technologies for applications in the environmental field. Photocatalysis is widely proposed for water disinfection (Rago et al., 2014), de-coloration of industrial dyes, air pollutants removal and could represent an alternative to the traditional activated carbon treatment of water deriving from processes with high amount of soluble organic compounds (de Caprariis et al., 2017). Among this latter the decontamination of polluted water streams containing traces of pharmaceutical compounds is a major challenge (Iovino et al., 2016; Iovino et al., 2016). Photocatalytic remediation is based on redox reactions of electrons and holes generated from semiconductors by bandgap excitation under light irradiation with water, oxygen, and organic (or inorganic) species. The semiconductors photoresponse under light irradiation (and the consequent photooxidation process), is then primarily dependent on the band gap value and on the energy input from the radiation, which must be sufficient to produce energy-rich electron–hole pairs.
Many efforts have been made by the scientific community for the improvement of the synthesis methods for the production of semiconductor oxide nanoparticles due to their unique properties in the photocatalysis. Among them, titanium dioxide (TiO_2) nanoparticles have drawn much attention recently in the field of photocatalysis. Titania, in fact, is a wide bandgap semiconductor with many interesting properties such as, high light emission, low production cost, chemical stability, non-toxicity and tailorable electronics properties and morphology. These properties have contributed to the use of TiO_2 nanoparticles in a variety of applications in different industries sectors. For example, TiO_2 films grown on various substrates promise to have a high commercial potential in the environmental applications such as self-cleaning, anti-bacterial, and

Please cite this article as: Scarsella M., Bracciale M.P., De Caprariis B., De Filippis P., Petrullo A., Pronti L., Santarelli M.L., 2017, Improved photocatalytic properties of doped titanium–based nanometric oxides, Chemical Engineering Transactions, 60, 133-138
DOI: 10.3303/CET1760023

waste water purification containment (Wanga et al.,1998). To extend its applicability, the ease of production and reproducibility has to be secured in terms of production cost and product quality.
One serious limit of this oxide is the wide band gap of its two main forms, corresponding to 3.18 eV and 3.02 eV for anatase and rutile respectively. Therefore, with pure TiO_2 it is possible to obtain a high photoresponse and degradation efficiency only under UV light irradiation, that is only 3 to 4% of the solar radiation, so limiting its environmental large-scale applications under diffuse daylight. Consequently, different strategies, such as metal and non-metal doping and co-doping, sensitizing the TiO_2 surface, and their combination by means of different synthesis routes are being studied.
Another important approach is based on the synergistic combination of TiO_2 with a different semiconductor metal oxide, in the form of mixed oxides composites or as binary/ternary oxides systems (such as perovskites, or pyrochlores) that can lead to an improved photocatalytic efficiency under visible light (λ >400nm), presenting a narrow bad gap, broadening the band absorbance or modifying the light-mediated surface redox reactions. Furthermore, to improve the photocatalytic activity of a material it is fundamental to take into account morphological parameters such as specific surface-area, average pore size, pore volume and distribution, crystallites average size and the amount of different phases. Accordingly, nanocrystalline materials with high surface area is imperative for application with high photocatalytic activity under visible light irradiation. In this work the photocatalytic efficiency of titanium-based oxides systems containing bivalent metals and prepared by a simple sol-gel method was investigated, evaluating the degradation of methylene blue as model compound under UV and visible light irradiation. The obtained results were also correlated with the morphological and optical properties of the developed products by X-ray diffraction (XRD), scanning electron microscopy (SEM) and diffuse reflectance UV–vis spectroscopy.

2. Materials and methods

2.1 Photocatalyst preparation

Titania-doped nanopowders were produced using a sol-gel method. Two photocatalysts were synthesized Ba-TiO_2 and Sr-TiO_2 were the metal load is for both 1 % by weight. The starting materials were Titanium(IV) butoxide (reagent grade, 97 %), Strontium nitrate (99 %) and Barium nitrate (99 %), all the products were purchased from Sigma-Aldrich. To a solution of the selected metal nitrate in methanol (1.5 mmol/L) kept under continuous stirring was added dropwise a solution of titanium butoxide in ethanol (volumetric ratio: 0.25) in order to obtain a metal concentration in the titanium doped-oxide of 1 % by weight. The formation of the gel phase takes place keeping the precursor solution under continuous stirring at ambient temperature for 24 hours. Then the obtained gel was dried at 80 °C overnight, grinded and then calcined in air at 350 °C. Three different calcination times were tested for the same sample, 3, 6 and 9 hours in order to evaluate the influence of this parameter on the TiO_2 structure and thus on the photocatalytic activity.

2.2 Photocatalyst characterization

The anatase and rutile contents and crystallite sizes of the materials prepared in this study were determined via quantitative X-ray diffraction (XRD) using a Philips Analytical PW1830 X-ray diffractometer, equipped with Cu Kα (1.54056 Å) radiation, in the 2θ range from 2.5 to 70° with a step size of 0.02° and a time for step of 1.25 min. The data were collected with an acceleration voltage and applied current of 40 kV and 30 mA, respectively. The average crystallite sizes were calculated with the Scherrer's equation and the fraction of phases in the mixture by method reported by Di Paola et al. (Di Paola et al., 2014).
Diffuse reflectance UV–Vis spectra (UV-vis-DRS) to determine the band gap of the photocatalysts were carried out on a dry pressed disk sample using a spectrophotometer (AvaSpec-2048, Avantes) equipped with a halogen lamp with a tungsten filament (HL-2000 FHSA, Avantes) as light source. The spectrometer is composed by a diffraction grating of 300 lines/mm, blazed at 500 nm, and a CCD linear sensor (2048 pixels). The reflectance measurements were collected with a spectral resolution of 0.8 nm between 300 and 1100 nm with an integration time of 40 ms and 100 scans. The samples were illuminated at 45° with a bifurcated fiber (diameter of 600 μm), connected to the halogen lamp, and the reflected light was collected with a 200 μm diameter fiber at 90° respect to the surface (45°/0° geometry). A Spectralon standard (Labshere SRS-99-010, 99 % reflectance) was taken as reference for the reflectance spectra.
BET-surface area was calculated from the BET plot acquired using Quantasorb surface area analyzer (Quantachrome Corporation) and helium-nitrogen gas mixture.
High Resolution-Field Emission Scanning Electron Microscopy (HR-FESEM, AURIGA Zeiss) images of the most active TiO_2 among the synthesized catalysts was recorded at 150 kV.

2.3 Photodegradation experiments

The photocatalytic activity of the catalysts was evaluated by measuring the decrease in concentration of methylene blue dye in a water reaction solution under UV and visible irradiation. The performances of the prepared catalysts were compared with the performances of Degussa P25 titanium dioxide purchased by Sigma-Aldrich (nanopowder with primary particle size of 21 nm and surface area of 35-65 m^2/g).
The experimental tests were performed in pyrex reactors opened to air having a capacity of 100 mL. the irradiation was provided by UV (365 nm and $irradiance_{max}$ = 2.5 W/m^2 at 6 cm to the surface; VL215-L, Consort) and visible light Led lamp (400 < λ < 800 nm and $irradiance_{max}$ = 5.5 W/m^2 at 6 cm to the surface; Superstar Classic-A100, Osram). An amount of 50 mL of 13 mg/l of methylene blue aqueous solution was kept in constant agitation, insured by magnetic stirrer, with 0.045 g of the prepared catalysts and 0.015 g of Degussa TiO_2 due to the much higher surface area of this material. Before starting the illumination phase the suspensions were stirred continuously for 30 min in the dark in order to evaluate the adsorption of the materials. The irradiation time was for all the tests 1 hour. After the irradiation, the catalyst was separated by centrifugation from the aqueous solution prior to analysis.
The concentration of methylene blue dye in the aqueous solution was measured at λ_{max} = 664 nm with an UV-visible spectrophotometer (Sequoia-Turner, 340) equipped with a quartz cell having a path length of 1 cm. The concentration of methylene blue in the solution was determined using a calibration curve of methylene blue (concentration *vs* absorbance) obtained with known concentrations.

3. Results and discussion

The characteristics of catalysts including anatase/rutile phases, crystallite size, surface area and optical band gap are summarized in Table 1.

Table 1: Catalyst characteristics.

	UV-vis band gap		XRD		BET
	Eg direct eV	Eg indirect eV	Crystallite size nm	Phase[a] wt %	Surface Area m^2/g
Ba-TiO_2_350 °C -3h	2.45	3.10	A: 16	A: 47.11; Am: 52.87	60.94
Ba-TiO_2_350 °C -6h	2.72	3.13	A: 16	A: 66.96; Am: 33.04	73.36
Ba-TiO_2_350 °C -9h	2.81	3.16	A: 14	A: 97.60; Am: 2.40	77.49
Sr-TiO_2_350 °C -3h	2.91	3.22	A: 13	A: 60.39; Am: 39.61	63.45
Sr-TiO_2_350 °C -6h	2.91	3.22	A: 11	A: 60.68; Am: 39.32	58.40
Sr-TiO_2_350 °C -9h	2.85	3.20	A: 10	A: 63.07; Am: 36.93	56.57
P25	2.99	3.15	A: 19; R: 28	A: 70.80; R: 17.40; Am: 11.80	52.66

[a]determined as reported by Di Paola et al. [2]: A, R and Am denote anatase, rutile, and amorphous, respectively.

The average crystallite size of nanopowders (*d*) was determined from the XRD patterns, according to the Scherrer's equation:

$$d=k\lambda/\beta\cos\theta \quad (1)$$

where *k* is a constant (shape factor, about 0.9), *λ* the X-ray wavelength (0.154 nm), *β* the full width at half maximum (FWHM) of the most intense diffraction peak and *θ* is the diffraction angle. The values of *β* and *θ* of anatase and rutile phases were taken from anatase (101) and rutile (110) planes diffraction lines, respectively (Figure 1) (Alijani et al., 2017).
Figure 1 reports the X-ray diffraction patterns of the catalysts synthesized in this work. All the catalysts samples consisted of only anatase, whereas Degussa P25 consisted of both anatase and rutile. Phases related to Ba and Sr were not significantly detected in any of the samples due to their low concentration levels and hence their doping did not result in any significant change in the phase crystallinity. Ba and Sr did not show any phase changes suggesting that aggregates might have been formed on the crystal borders and on

the surface of the photocatalyst, thus promoting visible light absorption, as discussed earlier (Naraginti et al., 2015). As shown in Table 1, the anatase crystallite size decrease with calcination time for all catalyst.
In order to evaluate the crystallinity of the samples XRD diffractograms were recorded for mixtures of TiO_2 and CaF_2 (50 wt %). By determining the ratio between the areas of anatase (101) or rutile and CaF_2 (220) peaks the amount of crystalline and amorphous phases present in the samples was determined (Di Paola et al., 2014).
Degussa P25 is close to being fully crystalline consisting of ~ 71 % anatase and ~ 17 % rutile with the amount of amorphous part in agreement with the value reported by Di Paola et al. (Di Paola et al., 2014). Among the synthesized samples, a higher crystallinity percentage (~ 98 %) was found for the sample Ba-TiO_2 calcined at 350 °C for 9 hours whereas only 47 % was the crystallinity achieved for Ba-TiO_2 warmed at the same temperature for 3 hours. The Sr-TiO_2 series show a constant crystallinity around 60 % with a slight variation due to the calcination time.
The bandgap energy (Eg) of semiconductors can be evaluated from the diffuse reflectance (UV-vis-DRS) spectrum. It is established that TiO_2 has direct and indirect band gaps (Janitabar-Darzi et al., 2009). The two different kinds of transitions can be distinguished by their energy dependence of the optical absorption coefficient (α) near the absorption edge. The optical gap value is estimated relying on the Kubelka–Munk method combined with the Tauc relation (Alijani et al., 2017).

$$[(\alpha h\nu) = B\,(h\nu - Eg)^{n}] \qquad (2)$$

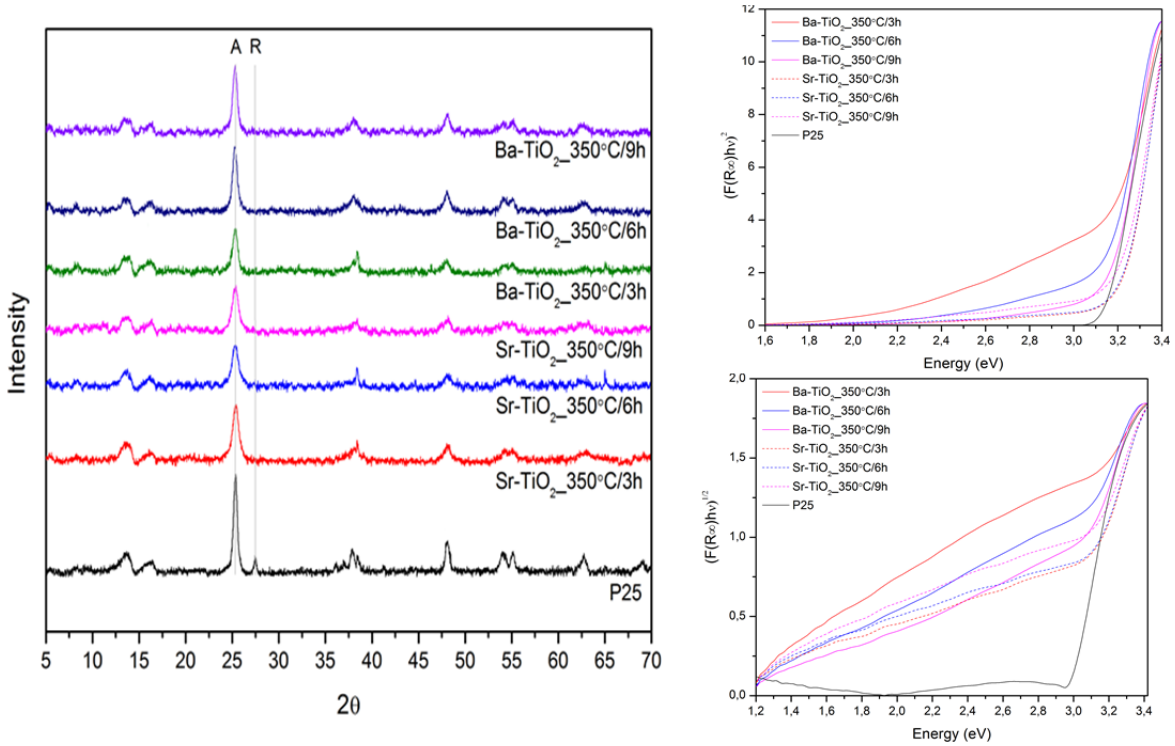

Figure 1: Sx: XRD patterns of the used photocatalysts; Dx: Indirect and direct band gap of catalysts.

where *B* is a constant, *α* is absorption derived by the remission function of Kubelka-Munk $F(R\infty)$ ($\alpha = k(\lambda)/s(\lambda) = (1- R\infty)^2/2R\infty$. Here, $R\infty$ is defined as $R\infty = R_{sample}/R_{reference}$ with $R_{reference}$, the diffuse reflectance measured for the Spectralon standard), *Eg* is the average band gap of the material and *n* depends on the type of transition (*n* = 1/2 for direct transmission and *n* = 2 for indirect transmission) (Lopez et al., 2012), *h* is the Plank's constant ($6.626\ 10^{-34}$ J s), and *v* is the frequency of photons. The direct and indirect average bandgap transition energies were estimated by the intercepts at $\alpha = 0$ of the linear portion of the $(\alpha h\nu)^2$ or $(\alpha h\nu)^{1/2}$ versus *hv* of plots, respectively, as shown in Figure 1.
It was observed that the doping of TiO_2 with alkaline earth metals (Ba and Sr) resulted in a decrease in the band energy (see also Table 1) and an increase in the wavelength (red shift). These results indicate that Sr

and Ba doped TiO_2 nanoparticles have greater possibility to exhibit a higher photocatalytic activity in the visible region.

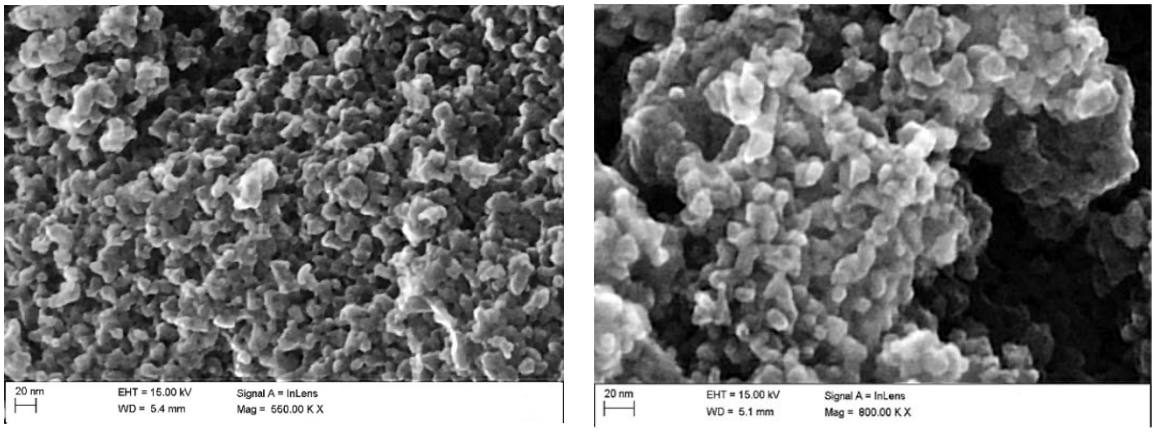

Ba-TiO_2_350C-6h Sr-TiO_2_350C-3h

Figure 2: FESEM images of the catalysts.

A representative SEM images in Figure 2 shows an uneven distribution of agglomerated particles with spherical shape and an average size in agreement with those determined from XRD.
The results of the methylene blue removal are reported in Table 2 for UV and visible light irradiation, the obtained values are compared with the results obtained by the Degussa P25 in the same conditions. The removal percentage was calculated as:

$$\% \text{ removal} = (C_{in} - C_{out})/C_{in} \times 100 \quad (3)$$

where C_{in} and C_{out} are the concentration calculated by the adsorption data measured with the spectrophotometer at the beginning and the end of the tests. All the powders were active for the photodegradation of the substrate under UV light although the efficiency of P25 was still higher.

Table 2: Photocatalytic activity on % degradation of methylene blue dye solution in the presence of UV and visible light

	UV %	Visible %
Ba-TiO_2_350C-3h	70.10	9.67
Ba-TiO_2_350C-6h	86.25	14.60
Ba-TiO_2_350C-9h	91.12	5.88
Sr-TiO_2_350C-3h	97.56	12.90
Sr-TiO_2_350C-6h	92.62	9.78
Sr-TiO_2_350C-9h	90.48	9.70
P25	98.90	9.91

Under visible light irradiation, the prepared Ba and Sr doped TiO_2 calcined at 350 °C for 6 and 3 hours respectively, exhibit higher degradation efficiency as compared to Degussa P25. This can be due to the reduced bandgap and to the prevention of electron–hole recombination owing to TiO_2 doping. Indeed, as previously reported, alkaline earth metal ions (Sr and Ba) doping in TiO_2 acts as an electron trap and leads to suppression of electron and hole recombination (Sood et al., 2015).
It is known that the photocatalytic activity of doped TiO_2 generally increases with higher crystallization degree, lower crystallite size and lower band gap. The combination of these parameters gives to the Ba-TiO_2 350C-6h the best performances under visible light irradiation.

4. Conclusions

TiO_2 nanoparticles doped with alkaline earth metal ions (Sr and Ba) have been synthesized by a simple sol-gel method and were calcined at 350 °C in air for 1, 3 and 9 h. The TiO_2 nanopowders obtained consist of anatase and the size of the crystallites, depending on the calcination time, is always smaller than that of Degussa P25. The prepared catalysts show excellent crystalline, morphological and optical properties.
The sunlight assisted photocatalytic experiments have been performed for the degradation of methylene blue dye. Photo-degradation of about 15 % within 60 min was observed for Barium doped TiO_2 calcined at 350 °C for 6 hours due to its band-gap, crystallinity and particle size, all contributing to the enhanced photocatalytic activity. The obtained results are an important first step for the development of alkaline earth metal doped TiO_2 nanocatalysts to be used in the photocatalytic degradation of organic contaminants present in wastewater under solar light irradiation.

Reference

Alijani M., Kaleji B.K., 2017, Optical and structural properties of TiO2 nanopowders with Ce/Sn doping at various calcination temperature and time, Opt. Quantum Electron. 49, 1-16.

de Caprariis B, De Filippis P, Hernandez A.D., Petrucci E., Petrullo A., Scarsella M., Turchi M., 2017, Pyrolysis wastewater treatment by adsorption on biochars produced by poplar biomass, J. Environ. Manage., 197, 231-238.

de Caprariis B, De Filippis P, Petrullo A, Scarsella M., 2015, Olive oil residue gasification and syngas integrated clean up system, Fuel, 158, 705-710.

de Caprariis B, Bassano C., Deiana P., Palma V., Petrullo A., Scarsella M., De Filippis P., 2014, Carbon dioxide reforming of tar during biomass gasification, Chemical Engineering Transactions, 37, 97-102. DOI: 10.3303/CET1437017.

Di Paola A., Bellardita M., Palmisano L., Barbieriková Z., Brezová V., 2014, Influence of crystallinity and OH surface density on the photocatalytic activity of TiO2 powders, J. Photochem. Photobiol. A Chem. 273, 59–67.

Iovino P., Chianese S., Canzano S., Prisciandaro M., Musmarra D., 2016, Ibuprofen photodegradation in aqueous solutions, Environ. Sci. Pollut. R. 23, 22993-23004.

Iovino P., Chianese S., Canzano S., Prisciandaro M., Musmarra D., 2016, Degradation of Ibuprofen in aqueous solution with UV Light: the effect of reactor volume and pH, Water Air Soil Poll. 227, 194-194.

Janitabar-Darzi S., Mahjoub A.R., Nilchi A., 2009, Investigation of structural, optical and photocatalytic properties of mesoporous TiO2 thin film synthesized by sol-gel templating technique, Phys. E Low-Dimensional Syst. Nanostructures. 42, 176–181.

Lopez R., Gomez R., 2012, Band-gap energy estimation from diffuse reflectance measurements on sol-gel and commercial TiO2: A comparative study, J. Sol-Gel Sci. Technol. 61, 1–7.

Naraginti S., Thejaswini T.V.L, Prabhakaran D., Sivakumar A., Satyanarayana V.S.V., Arun A.S., 2015, Prasad Enhanced photo-catalytic activity of Sr and Ag co-doped TiO2 nanoparticles for the degradation of Direct Green-6 and Reactive Blue-160 under UV & vis, Spectrochim. Acta A 149, 571-579.

Rago I., Chandraiahgari C.R., Bracciale M.P., De Bellis G., Zanni E., Cestelli Guidi M., Sali D., Broggi A., Palleschi C., Sarto M.S., Uccelletti D., 2014, Zinc oxide microrods and nanorods: Different antibacterial activity and their mode of action against Gram-positive bacteria, RSC Adv. 4, 56031-56040.

Serpone N., Lawless D., Khairutdinov R., 1995, Size Effects on the Photophysical Properties of Colloidal Anatase TiO2 Particles: Size Quantization versus Direct Transitions in This Indirect Semiconductor, J. Phys. Chem. 99, 16646–16654.

Sood S., Umar A., Mehta S.K., Sinha A.S.K., Kansal S.K., 2015, Efficient photocatalytic degradation of brilliant green using Sr-doped TiO2 nanoparticles, Ceram. Int. 41, 3533-3540.

Wanga T., Wanga H., Xu P., Zhao X., Liu Y., Chao S., 1998, The effect of properties of semiconductor oxide thin films on photocatalytic decomposition of dyeing waste water, Thin Solid Films 334, 103-108.